NEARSHORE MIXING AND DISPERSION

IB A. SVENDSEN and UDAY PUTREVU

RESEARCH REPORT NO. CACR-94-08

February 1994

CENTER FOR APPLIED COASTAL RESEARCH

Ocean Engineering Laboratory
University of Delaware
Newark, Delaware 19716

NEARSHORE MIXING AND DISPERSION

Ib A. Svendsen & Uday Putrevu
Center for Applied Coastal Research
Department of Civil Engineering
University of Delaware
Newark, Delaware 19716

Abstract

Longshore currents have in the past been analyzed assuming that the lateral mixing could be attributed to turbulent processes. It is found, however, that the mixing that can be justified by assuming an eddy viscosity $\nu_t = \ell\sqrt{k}$ where ℓ is the turbulent length scale, k the turbulent kinetic energy, combined with reasonable estimates for ℓ and k is at least an order of magnitude smaller than required to explain the measured cross-shore variations of longshore currents.

In the present paper, it is shown that the nonlinear interaction terms between cross- and longshore currents represent a dispersive mechanism that has an effect similar to the required mixing. The mechanism is a generalization of the one-dimensional dispersion effect in a pipe discovered by Taylor (1954) and the three-dimensional dispersion in ocean currents on the continental shelf found by Fischer (1978).

Numerical results are given for the dispersion effect, for the ensuing cross-shore variation of the longshore current and for the vertical profiles of the longshore currents inside as well as outside the surf zone. It is found that the dispersion affect is at least an order of magnitude larger than the turbulent mixing and that the characteristics of the results are in agreement with the sparse experimental data material available.

1 INTRODUCTION

Lateral mixing on gently sloping beaches plays an important role in the distribution of nearshore currents. The possible mechanisms responsible for the mixing have been discussed in the literature even before the concept of radiation stress was introduced and shown to be the primary forcing for the nearshore circulation (Harris, et al. 1963) and later by Inman et al. (1974), Bowen & Inman (1974) and Battjes (1975). In particular, the longshore

currents on a long straight coast have been analyzed so extensively that one would expect to find little new to add to the topic. In the present paper, however, we analyze the effect of current dispersion caused by the nonlinear interaction between the wave generated cross- and longshore currents. This is an extension of the three dimensional current pattern studied by Svendsen & Lorenz (1989) who neglected the non-linear current interactions. We find that this interaction includes a mechanism that has an effect similar to the traditional turbulent mixing, but even inside the surf zone is an order of magnitude stronger than the mixing that can be justified on the basis of the information we have about turbulence in the nearshore region. Thus, it is suggested that the unrealistically strong mixing that normally is assumed in numerical models of longshore currents in order to fit experimental observations can in fact be attributed to the dispersive effect of the vertical structure of the nearshore currents.

When waves approach the shore and break, they exert a net force on a water column due to the decrease in radiation stress (Longuet-Higgins & Stewart 1960, 64). The cross-shore component of this force is, in average over the depth, balanced by a pressure gradient caused by a slope in the mean water surface which results from a substantial wave setup in the surf zone. Due to the unequal distribution over depth of the forces involved, this mechanism also creates a cross-shore circulation which is fed by the shoreward mass flux in the breaking waves. On a coast with no net cross-shore transport, this leads to a strong vertical current shear with a seaward oriented undertow current which is particularly strong near the bottom (Svendsen 1984).

In the longshore direction, the longshore component S_{xy} of the net radiation stress on the water column is in the average balanced by a mean bottom shear stress τ_{by} which is created by a longshore current. In addition, a lateral mixing process creates shear stresses

which are usually described by a gradient law of the type

$$\tau_{xy} = \rho \nu_{tx} \frac{\partial V}{\partial x} \tag{1.1}$$

where $V(x)$ is the longshore current along the shore normal x-axis and ν_{tx} is a turbulent eddy viscosity (Bowen, 1969; Thornton, 1970 and Longuet-Higgins, 1970). Hence, the equation for $V(x)$ reads

$$\rho \frac{\partial}{\partial x}\left(\nu_{tx} h \frac{\partial V}{\partial x}\right) - \tau_{by} - \frac{\partial S_{xy}}{\partial x} = 0 \tag{1.2}$$

where τ_{by} is $\tau_{by}(V)$. As indicated by Longuet-Higgins (1970; L-H in the following), the singular nature of (1.2) makes the mixing term crucial in creating predictions of $V(x)$ that have resemblance with measured current distributions across the surf zone.

The lateral mixing coefficient ν_{tx} has frequently been expressed as $\nu_{tx} = Nx\sqrt{gh}$ which on a plane beach can also be written as

$$\nu_{tx} = C_x h \sqrt{gh} \tag{1.3}$$

L-II found that values of $N = 0.01$–0.02 were required for the solutions of (1.2) to fit measured values of $V(x)$, and this order of magnitude of ν_{tx} has been confirmed several times since.

On the other hand, Svendsen et al. (1987) found by comparing measurements for undertow on a 1/35 beach with model predictions, that in the vertical direction the vertical mixing coefficient

$$\nu_{tz} = C_z \, h \, \sqrt{gh} \tag{1.4}$$

with $C_z \sim 0.01$. This figure has been confirmed by Okayasu (1989).

A natural hypothesis is to assume that the mixing is caused by the turbulence which is abundant due to the wave breaking. We may then express ν_t as

$$\nu_t = \ell \sqrt{k} \tag{1.5}$$

where k is the turbulent kinetic energy and ℓ a characteristic length scale for the turbulence. Based on measurements, Svendsen (1987) estimated $k = O(0.05\sqrt{gh})$. With $C_z = 0.01$, this then corresponds to $\ell_z = O(0.2h)$ which seems reasonable. In contrast, $N \sim 0.01$–0.02 will, on a beach with slope 1/35, correspond to $C_x \sim 0.35$–0.70 (or $\ell_x = O\ (1.6\text{–}3.2h)$). Altough there clearly could be a difference between the vertical and horizontal structure of the turbulence, a factor of 35–70 between the respective mixing coefficients seems unlikely.

In fact, it would be a more reasonable assumption that the characteristic length scale ℓ in the horizontal and vertical directions are similar (so that $\nu_{tx} = \nu_{tz} = \nu_t$ or $C_x = C_z$). For clarity, we will distinguish between ν_{tx} and ν_{tz} in the derivations in section 2, although we will in the numerical examples and comparisons assume that the two are equal.

Thus, there is an order of magnitude difference between the ν_t required to predict the measured cross shore variation of longshore currents and the vertical variation of undertow, respectively.

As an illustration, Fig. 1 shows calculations of the longshore current distribution $V(x)$ with ν_{tx} based on $C_x = 0.01$ and 0.35, respectively. For simplicity, the analytical L-H solution has been used in the computation.

In the present paper, we first analyze the effect of the vertical variation of the cross-shore and longshore currents and show (Section 2) that these variations actually represent a strong horizontal mixing or dispersion mechanism. In Section 3, numerical results for the dispersion coefficient are given and compared with the mixing coefficient that can be reasonably justified on the basis of turbulent measurements and measured undertow profiles. Section 4 shows computations of velocities and comparison with Visser's (1984) laboratory measurements and Section 5 contains further discussion and comparison with the possible mixing caused by shear instabilities and by the time varying breaker characteristics of storm

waves as observed in field experiments.

2 SOLUTION FOR A LONG STRAIGHT BEACH

On a long straight coast with gently sloping bottom, we consider steady, longshore uniform flow of waves incident at an angle to the shore normal and the longshore currents generated by these waves. We use an x, y, z coordinate system with x, y (x shore normal) at the undisturbed still water level SWL, z vertically upwards. The undisturbed water depth is $h_0(x)$ and the mean water surface elevation is $\bar{\zeta}(x)$.

The depth integrated, wave averaged equation for longshore momentum in this situation can be written

$$\frac{d}{dx}\overline{\int_{-h_0}^{\zeta}(\rho uv - \tau_{xy})\,dz} + \tau_{by} = 0 \tag{2.1}$$

Here, u, v represent x, y components of combined wave and current velocities, $\tau_{xy} = -\rho\overline{u_t v_t}$ the turbulent Reynolds stresses. $\overline{}$ refers to the time averaging (over a wave period) and τ_{by} is the mean longshore bottom shear stress.

Depth integrated, wave averaged conservation of mass implies

$$\overline{\int_{-h_0}^{\zeta} u dz} = 0 \tag{2.2}$$

For convenience, we introduce dimensionless variables given by

$$x', u', z', h' = (x, y, z, h)\, h_b^{-1} \tag{2.3}$$

$$(u', v') = (u, v)\, c_0^{-1}$$

$$\nu_t' = \nu_t (h_b c_0)^{-1} \tag{2.4}$$

$$\tau' = \tau(\rho\, c_0^2)^{-1}$$

where $c_0 = (g h_b)^{1/2}$, and h_b is a characteristic depth (e.g. the breaker depth).

The velocities u', v', w' may be divided into a wave part u'_w, v'_w, w'_w (with zero time average below wave trough level) and a current part U', V', W'. Observational evidence indicates that whereas $U' \ll 1$, the variation of U' over depth is $O(U')$. Conversely, V' may be $O(1)$ but shows little variation over depth. Thus we assume the motion can be represented by

$$\begin{aligned} u'(x,z) &= u'_w(x,z) + U'(x,z) \\ v'(x,z) &= v'_w(x,z) + V'_0(x) + V'_1(x,z) \end{aligned} \tag{2.5}$$

where $V'_1 \ll V'_0 = O(1)$, and $U' \ll 1$.

In conjunction with what is often the case on real beaches, it is assumed that the height to depth ratio of the breaking and near breaking waves will be $O(1)$ so that u'_w, $v'_w = O(1)$.

Finally, we assume that the Reynolds stress τ'_{xy} can be represented by

$$\tau'_{xy} = \nu'_{tx} \frac{\partial V'}{\partial x'} \tag{2.6}$$

where

$$V' = V'_0 + V'_1 \tag{2.7}$$

Introducing (2.5) into (2.2) leads to

$$\int_{-h'_0}^{\overline{\zeta'}} U'_1 \, dz' = -\overline{\int_{-h'_0}^{\zeta'} u'_w \, dz'} = -\overline{\int_{\zeta'_t}^{\zeta'} u'_w \, dz'} \tag{2.8}$$

where ζ'_t is the elevation of the wave trough and the latter equality utilizes that $\overline{u'_w} = 0$ below trough level.

The gentle slope assumption implies that $\partial/\partial x' \ll 1$. Therefore, when substituting (2.6) and (2.7) into (2.1), the V'_1 contribution to the τ_{xy} term can be neglected and we get, using (2.8)

$$\frac{d}{dx'}\left(\int_{-h'_0}^{\overline{\zeta'}} \nu'_{tx} dz' \frac{dV'_0}{dx'}\right) - \tau'_{by} - \frac{d}{dx'}\overline{\int_{-h'_0}^{\zeta'} U'_1 V'_1 + u'_w V'_1 + v'_w U'_1 dz} = \frac{dS'_{xy}}{dx'}. \tag{2.9}$$

Eq. 2.8 can be used to further transform the third term in (2.9) as

$$\overline{\int_{-h_0'}^{\zeta'} (U_1'V_1' + u_w'V_1' + v_w'U_1')\,dz'} \cong \overline{\int_{-h_0'}^{\zeta'} (U_1'(V_1' - V_{1s}') + v_w'U_1')\,dz} \tag{2.10}$$

where $V_{1s}' = V_1'(\overline{\zeta'})$.

The vertical variation of the longshore current is given by the y-component of the Reynolds' equations. Introducing (2.5) directly, that equation may be written after averaging over a wave period

$$\frac{\partial}{\partial z'}\tau_{zy}' = \frac{\partial}{\partial x'}\overline{u_w'v_w'} + \frac{\partial}{\partial z'}\overline{v_w'w_w'} + U_1'\frac{\partial V'}{\partial x'} + W'\frac{\partial V_1'}{\partial z'} \tag{2.11}$$

Here the last term is negligible, and in the third term on the right hand side the small shear in the longshore current ($V_1' \ll V_0'$) implies that we may approximate $\partial V'/\partial x'$ by dV_0'/dx'.

The turbulent shear stress τ_{zy} is described by means of an eddy viscosity as

$$\tau_{zy}' = \nu_{tz}'\frac{\partial V_1'}{\partial z'} \tag{2.12}$$

At the bottom, this leads to the boundary condition that links the bottom shear stress τ_{by} to the bottom velocity V_b' (section 3).

Eq. (2.11) then becomes

$$\frac{\partial}{\partial z'}\left(\nu_{tz}'\frac{\partial V_1'}{\partial z'}\right) = \frac{\partial}{\partial x'}\overline{u_w'v_w'} + \frac{\partial}{\partial z'}\overline{v_w'w_w'} + U_1'\frac{dV_0'}{dx'} \tag{2.13}$$

Similarly U_1' satisfies the equation

$$\frac{\partial}{\partial z'}\left(\nu_{tz}'\frac{\partial U_1'}{\partial z'}\right) = \frac{\partial}{\partial x'}\left(\overline{\zeta'} + \overline{u_w'^2}\right) + \frac{\partial}{\partial z'}\overline{u_w'w_w'} \tag{2.14}$$

It is convenient to define

$$\begin{aligned} \alpha_x' &= \frac{\partial}{\partial x'}\left(\overline{\zeta'} + \overline{u_w'^2}\right) + \frac{\partial}{\partial z'}\overline{u_w'w_w'} \\ \alpha_y' &= \frac{\partial}{\partial x'}\overline{u_w'v_w'} + \frac{\partial}{\partial z'}\overline{v_w'w_w'} \end{aligned} \tag{2.15}$$

Returning from now on to dimensional variables, we can determine directly the $V_1 - V_{1s}$ needed for the integral in (2.10) by integrating (2.13). Introducing the definitions

$$a_y(z) = \int_z^{\bar{\zeta}} \frac{1}{\nu_{tz}} \int_{-h_0}^{z} \alpha_y dz dz \tag{2.16a}$$

$$b_y(z) = \frac{\tau_{by}}{\rho} \int_z^{\bar{\zeta}} \frac{dz}{\nu_{tz}} \tag{2.16b}$$

$$A(z) = \int_z^{\bar{\zeta}} \frac{1}{\nu_{tz}} \int_{-h_0}^{z} U_1 dz dz \tag{2.16c}$$

we may express $V_1 - V_{1s}$ as

$$V_{1s} - V_1 = a_y(z) + b_y(z) + A(z)\frac{dV_0}{dx} \tag{2.17}$$

A similar solution is obtained for U_1, namely

$$U_1 = a_x(z) + b_x(z) + U_b \tag{2.18}$$

where

$$a_x(z) = \int_{-h_0}^{z} \frac{1}{\nu_{tz}} \int_{-h_0}^{z} \alpha_x dz dz \tag{2.19}$$

$$b_x(z) = \frac{\tau_{bx}}{\rho} \int_{-h_0}^{z} \frac{dx}{\nu_{tz}} \tag{2.20}$$

U_b is determined so that (2.2) is satisfied.

The integral (2.10) may then be determined as

$$\begin{aligned} \int_{-h_0}^{\bar{\zeta}} U_1(V_1 - V_{1s})dz + \overline{\int_{\zeta_t}^{\zeta} v_w U_1 dz} &= -\int_{-h_0}^{\bar{\zeta}} U_1 \, A \, dz \frac{dV_0}{dx} \\ &\quad - \int_{-h_o}^{\bar{\zeta}} (a_y(x) + b_y(z))\, U_1 dz + \overline{\int_{\zeta_t}^{\zeta} v_w \, U_1 \, dz} \end{aligned} \tag{2.21}$$

The nature of this result is more clearly illustrated if we define

$$D_c = \frac{1}{h} \int_{-h_0}^{\bar{\zeta}} U_1 \, A \, dz \tag{2.22}$$

or

$$D_c = \frac{1}{h}\int_{-h_0}^{\bar{\zeta}} U_1 \int_z^{\bar{\zeta}} \frac{1}{\nu_{tz}} \int_{-h_0}^{z} U_1 \, dz \, dz \, dz \tag{2.23}$$

and

$$F_1 = -\int_{-h_0}^{\bar{\zeta}} U_1 \int_z^{\bar{\zeta}} \frac{1}{\nu_{tz}} \int_{-h_0}^{z} \alpha_y \, dzdzdz + \overline{\int_{\zeta_t}^{\zeta} v_w \, U_s \, dz} \tag{2.24}$$

$$F_2 V_0 = -\frac{\tau_{by}}{\rho}\int_{-h_0}^{\bar{\zeta}} U_1 \int_z^{\bar{\zeta}} \frac{dz}{\nu_{tz}} \, dz \tag{2.25}$$

Using these definitions (2.10) may be written

$$\int_{-h_0}^{\bar{\zeta}} (U_1 V_1 + u_w V_1 + v_w U_1)\, dz = -D_c h \frac{dV_0}{dx} + F_1 + F_2 V_0 \tag{2.26}$$

and (2.9) becomes

$$\frac{d}{dx}\left(D_c h + \int_{-h_0}^{\bar{\zeta}} \nu_{tx} dz\right)\frac{dV_0}{dx} - \frac{\tau_{by}}{\rho} - \frac{d}{dx}(F_2 V_0) = \frac{1}{\rho}\frac{dS_{xy}}{dx} + \frac{dF_1}{dx} \tag{2.27}$$

Thus the current-current interaction can be expressed in terms of three additional terms in the depth integrated equation for longshore momentum, represented by D_c, F_1 and F_2. Of those, the D_c-term is by far the most important. As (2.27) shows, D_c acts as an additional mixing over and above that provided by the turbulent mixing ν_{tx}.

The structure of the expression (2.23) is similar to that obtained by Taylor (1954) for dispersion of dissolved matter in pipe flow. Similar results have been obtained by Elder (1959) for suspended pollutants in open channel flow and by Fisher (1978) for pollutants in ocean currents on the continental shelf. In the present situation it is (longshore) momentum itself that is being dispersed (for the simple case considered here) by the cross shore circulation. The dispersion also includes some additional terms represented by F_1 and F_2. Though smaller, the example in section 4 shows that their effect is not completely negligible.

As (2.10) shows, it may also be noticed that since the value of the interaction integrals only depends on $V_1 - V_{1s}$, not on the absolute value of the longshore current V, a precise

interpretation of V_0 is unnecessary for the derivation. Thus, V_0 may be defined as the depth mean longshore velocity, in which case $V_1(z)$ is completely analogous to $U_1(z)$. This is clearly the most natural definition of V_0 and V_1 as an interpretation of the ν_{tx}-term in (2.27) suggests. Alternatively, however, V_0 can also be the bottom velocity V_b in the longshore velocity profile in which case the evaluation of $\tau_b = \tau_b(V_b)$ becomes somewhat simpler.

3 NUMERICAL RESULTS

To illustrate the nature of the results, it is instructive to consider the special case of $\nu_{tx} = \nu_{tz}$ = constant over the depth, α_x, α_y similarly depth uniform, and waves at a small angle of incidence. In this case, the expressions for U_1 and $V_1 - V_{1s}$ can be written as

$$\begin{aligned} U_1 &= a_x\,\xi^2 + b_x\xi + U_b \\ V_1 - V_{1s} &= a_y\xi^2 + b_y\xi + A(\xi)\frac{dV_0}{dx} \end{aligned} \tag{3.1}$$

where

$$a_x = \frac{1}{2}\,\frac{\alpha_x}{\nu_{tz}} \quad ; \quad b_x = \frac{\tau_{bx}}{\rho\nu_{tz}} \tag{3.2}$$

$$a_y = \frac{1}{2}\,\frac{\alpha_y}{\nu_{tz}} \quad ; \quad b_y = \frac{\tau_{by}}{\rho\nu_{tz}} \tag{3.3}$$

are functions of the local meanwater depth $h(= h_0 + \bar{\zeta})$ through the way in which α_x, α_y, ν_{tz} are specified. For τ_b is used the simple linearized bottom friction

$$\tau_{bx} = \frac{2}{\pi}\rho\, f\, u_{wb}\, U_b \;\; ; \;\; \tau_{by} = \frac{1}{\pi}\rho\, f u_{wb}\, V_b \tag{3.4}$$

where f is a friction coefficient. This means that

$$b_x = \frac{2 f u_{wb}}{\pi\nu_{tz}} U_b = 2b\, U_b \;\; ; \;\; b_y = b\, V_b \tag{3.5}$$

where b is independent of U_b and V_b.

Defining U_m as the depth average of U_1, substituting (3.4) for τ_{bx}, and solving for U_b we get

$$U_b = U_m \cdot \frac{1 + \frac{1}{3}\frac{a_x h^2}{U_m}}{1 + \frac{bh}{2}} \tag{3.6}$$

which means $U(x,z)$ is completely determined.

Thus, the results for D_C, F_1 and F_2 can be expressed in terms of the parameters a_x, a_y which essentially represent the driving forces from the cross- and longshore radiation stresses, the parameter b linking ν_{tz}, the bottom friction parameter, and the wave motion together, and ν_{tz} the (vertical) eddy viscosity. U_m the depth averaged cross shore mean velocity is also a parameter.

We consider a plane beach with $h_{0x} = 1/30$. Typical values of U_m are $-(0.03 - 0.1)\sqrt{gh}$ (see e.g., Svendsen et al., 1987). From the same source, we assess α_x mainly on the basis of $d\bar{\zeta}/dx$ which in the surf zone typically is 10% of the undisturbed bottom slope, h_{0x}. Together with an estimated ν_{tz} of $0.01h\sqrt{gh}$ (2.20) then yields $a'_x \sim 0.15$ where $a'_x = a_x h^2/\sqrt{gh}$.

A realistic value of $f \sim 2 \cdot 10^{-2}$ (see e.g., Jonsson & Carlsen, 1976) gives $b' \sim 0.1$ where $b' = bh$.

These values are used as guidelines for the choice of parameter values for the numerical results shown below.

Fig. 2 shows the variation of $D'_C = D_C\,(\nu_{tz}/U_m^2 h^2)$ for $b' = b'_x = 0$ and $a'_x = 0$, 0.1 and 0.2 versus U_m. Although there clearly would be a dispersion effect even in the (unrealistic) case of a depth uniform undertow ($a_x = 0$), it is also clear that the usual depth variation of the undertow current ($a_x \neq 0$) greatly enhances the dispersion effect.

It may be mentioned that although D'_C grows as $U_m \to 0$, $D_C = (U_m^2 h^2/\nu_{tz})\,D'_C$ does

tend to zero in that limit as one would expect.

Fig. 3 shows the corresponding undertow profiles for the typical case of $U'_m = -0.06$.

In Figs. 2 and 3, b has been chosen to be zero. As has been found many times in the past (see particularly Svendsen & Hansen, 1988), the cross-shore bottom shear stress is quite small and exercises a very weak influence on the undertow velocity profile. Accordingly, it is found that curves for D_C for $b' = 0$, 0.1 and 0.2 (as representative values) can hardly be distinguished from one another. Consequently, the results in Fig. 2 for $b = 0$ (i.e., no mean cross-shore bottom shear stress) are representative for all reasonable values of b.

On the basis of Fig. 2, it is possible to give a crude estimate of the magnitude of D_C relative to ν_{tx}. For the case $\nu_{tz} = \nu_{tx}$, we get

$$\frac{D_C}{\nu_{tx}} = 0.5 \frac{U_m^2 h^2}{\nu_{tz}^2}$$

Here we have $U_m h = -Q_{wx}$, the wave mass flux, and a typical value of Q_{wx} is $0.06h\sqrt{gh}$. This suggests that $D_C/\nu_{tx} = O(10)$. In the example in Section 4, the D_C value turns out to be approximately 20 ν_{tx}. Hence, with $\nu_{tx} \sim 0.01h\sqrt{gh}$, we get $D_C = 0.20h\sqrt{gh}$.

The dispersion coefficient D_C depends on the turbulent eddy viscosity ν_{tz}, both directly and through U_1/U_m where ν_{tz} occurs both in a_x and b_x. The computations in Fig. 4 are for α_x in the range found for the experimental results analyzed by Svendsen et al. (1987), and with $b = 0$ (and hence $b_x = 0$). We see that in the range of ν_{tz} values between 0.01 and 0.03 $h\sqrt{gh}$ found in experiments, there is some variation of D'_C which grows with decreasing ν_{tz}. Since decreasing ν_{tz} represents decreasing turbulence from breaking, this will usually also be associated with a decline in the slope $d\bar{\zeta}/dx$ on the mean water level and hence, in Fig. 4, a reduction in α_x. No firm relation between the two parameters is available but it means that for real wave situations, the variation of D'_C with ν_{tz} will probably be much more moderate

than indicated by the α_x = const curves in Fig. 4.

4 CURRENT VELOCITIES ON A STRAIGHT COAST

In this section, equation (2.27) is solved numerically for the cross-shore variation $V_0(x)$ of the longshore velocity on a plane beach. The vertical profiles of U and V are obtained by solving (2.13) and (2.14).

The numerical results are developed under the simplifying assumption that sine wave theory is applicable for the calculation of the radiation stresses, and the assumption of a constant wave height to water depth ratio, γ, inside the surf zone. Outside the breaker point, Green's law of $H \propto h^{-\frac{1}{4}}$ is applied.

The distinction between wave conditions before and after breaking implies that at the breaking point ($h = h_b$), $\partial S_{xy}/\partial x$ jumps from zero outside the surf zone to a finite value at the breaking point and throughout the surf zone. Therefore, also, α_x and α_y, and hence a_x and a_y are discontinuous at $h = h_b$. Thus, the solution of (2.27) from the shoreline to deep water is established as a matched combination of the solutions inside and outside the breaker point with continuity in velocity and shear stress at h_b.

The boundary conditions used are

$$V_0 = 0 \quad \text{at} \quad \begin{cases} h = 0 \\ h/h_b \to \infty \end{cases} \tag{4.1}$$

To simplify the discussions, a'_x is assumed constant in the surf zone and equal to 0.15. This is in accordance with the assumption of γ = const which yields $d\bar{\zeta}/dx$ constant.

The longshore driving forces represented by α_y and S_{xy} are in the computations assumed to correspond to an angle of incidence for the waves of 11.3° at the breaker point which yields $v_w \sim 0.2\, u_w$ or $\overline{u_w v_w} \sim 0.2\, \overline{u_w^2}$, and γ is taken to be 0.7.

In the surf zone, the eddy viscosity ν_t is chosen as $0.01h\sqrt{gh}$. Outside the surf zone, ν_{tx} and ν_{tz} are expected to decrease as we move seaward. Very little information is available, even about the level of turbulent kinetic energy k in (1.5). Fig. 5 (from Nadaoka & Kondoh (1982)) shows the only known measurements of k outside the breaker point. The results indicate that although k deceases, the level of turbulence outside the breaker point is not negligible and does not seem to vanish completely even several times the surf zone width seaward of the breaker point. Based on these observations, we have used the following expression for $\nu_t = \nu_{tx} = \nu_{tz}$:

$$\nu_t = \begin{cases} 0.01h\sqrt{gh} & \text{inside surf zone} \\ [0.8(h/h_b)^{-4} + 0.2]\nu_{tb} & \text{outside surf zone} \end{cases} \tag{4.2}$$

where $\nu_{tb} = 0.01h_b\sqrt{gh_b}$ is the eddy viscosity at breaking.

In Fig. 6, we first make a comparison between computations with different parts of the solution in effect. Curve (a) represents a solution with ν_t given by (4.2) as the only source of mixing. Curve (b) in that figure represents the solution to Eq. (2.27). Finally, curves (c) and (d) represent solutions to (2.27) with F_1 and F_2 , respectively, equal to zero.

Inside the surf zone, the value of D_c used in Fig. 6 corresponds to about $20\nu_t$. Clearly, the effect of the dispersion is very significant.

The figure also shows that although F_1 and F_2 represent much weaker elements of the dispersion mechanism, they are not entirely negligible.

Simultaneously, with the computation of $V_0(x)$ the solutions for $U_1(x,z)$ and $V(x,z)$ are obtained as indicated earlier. The profiles for $V(x,z)$ are shown in Fig. 7 for the parameter values and assumptions outlined above.

These vertical profiles show an interesting shift near the breaker point. Outside that point, $\partial S_{xy}/\partial x = 0$ so that the currents are entirely driven by the dispersion mechanisms

and the (much weaker) turbulent mixing. The realism of these profiles is therefore a very sensitive indicator of the—at least qualitative—accuracy of the description of the dispersive mechanism.

For all positions, we find that $V(x,z)$ only vary slightly over the depth. Hence, as suggested earlier, the cross-shore distributions of V_0 in Fig. 6 are actually quite characteristic for the entire variation of the longshore current velocity field. Fig. 7 also shows, however, that from the shoreline and till a depth of about 0.8 h_b, the longshore current velocities increase slightly from the seabed towards the surface. From $h = 0.8h_b$ and seaward, this tendency is reversed and the maximum value of $V(z)$ now appears near the bottom.

Since a depth uniform V yields no dispersion effects whatsoever, this shift in the sign of $\partial V/\partial z$ indicates a similar shift in the sign of the dispersion effect, represented in the equation essentially by the change of sign of $\partial^2 V/\partial x^2$ around the same depth.

The solution to eq. 2.27 has also been compared with the measurements by Visser (1984). Fig. 8 shows both Visser's measured velocities for his experiment no. 4 (points), and computations with and without the dispersion in effect. Since very few of the parameters needed for the computations were actually provided by Visser, the set of values outlined above have been used with a few exceptions. Firstly, in recognition of the more violent breaking on the 1/20 slope of the experiment, the eddy viscosity ν_t has been chosen as $0.02\, h\, \sqrt{gh}$ inside the surf zone. Secondly, the errors introduced by using sine wave theory for the driving force S_{xy} (see Svendsen & Putrevu, 1993) and the uncertainty about the bottom friction, have been compensated by adjusting the bottom friction factor to $f = 0.017$ so that the measured and computed maximum velocities are of the same order. Finally, Visser's measurements show that in the region of interest outside the break point, the wave height is almost constant.

Fig. 9 shows the equivalent comprison with Visser's dye measurements of the longshore

velocities at three different levels over the depth (Visser, 1984). Measurements were taken at eight positions in the cross-shore direction corresponding to the eight points in Fig. 8 between $x = 1.20$ m and $x = 4.00$ m. Clearly, the predictions obtained by the very crude approximations of sine wave theory, constant H/h and C_x inside the surf zone, and the equally crude estimate of parameters outside the surf zone, do not quite fit the measurements. There may also be inaccuracies in the measurements due to the simple technique of dye injection. The trends, however, of changes in the vertical longshore profiles are clearly the same in the measured and computed results. Given the close connection between this feature and the dispersion mechanism, this qualitative agreement between measurements and theory seems very encouraging.

5 FURTHER DISCUSSIONS

Thus, with realistic values for the various parameters involved, the dispersion mechanism can be expected to be both of the right magnitude and variation to explain the substantial mixing which apparently is present, at least, in laboratory measurements.

Similar levels of mixing have been found, however, to be required to explain the cross-shore variation of field measurements of longshore currents, and for those conditions two alternative mechanisms have been suggested for providing such mixing.

Thus, Oltman-Shay et al. (1989) found that field measurements of longshore currents show temporal and spatial variations that may be interpreted as shear instabilities of such currents (Bowen & Holman, 1989). Such instabilities contribute a mixing mechanism which under certain conditions may be strong enough to account for the required mixing (Dodd & Thornton, 1990; Putrevu & Svendsen, 1992). Several factors, however, suggest that it is unlikely to be the commonly dominating mechanism. Firstly, Putrevu & Svendsen

(1992) found that for the theoretical instabilities investigated, the mixing only occurs inside the surf zone whereas there is virtually no mixing generated outside the breaker point by this mechanism. Secondly, no shear instabilities have been observed in the well controlled laboratory experiments where the same amount of actual mixing/disperion occurred as in the field. This could of course be because nobody was looking for such phenomena. However, estimates (Putrevu & Svendsen, 1992) suggest that the viscous threshold for development of the instabilities is probably not reached under typical laboratory conditions, so that it is in fact unlikely that instabilities occurred.

A second mechanism suggested for providing an effect similar to mixing is based on the fact that in the field, individual waves differ in height and period and hence break at different distances from the shoreline (Thornton & Guza, 1986). Both the variations in wave height and breaker point provide variations in longshore forcing, that averaged over some time, has an effect similar to a mixing.

The analysis of a large number of field measurements shown by Thornton & Guza clearly demonstrates the effect of such a variation. Their results show that when this mechanism is included the additional smoothing of the cross-shore variation of the longshore currents obtained by adding the traditional turbulent mixing is minor. Their results also show, however, that in a majority of the cases they analyzed, this mechanism falls far short of actually predicting the relatively large longshore current velocities measured around and seaward of the breaker point. Furthermore, this mechanism clearly is totally absent in the laboratory experiments with regular waves where the large mixing also occurs. It therefore seems that, although variation of the breaking point represents an important mechanism, it cannot explain all the observed aspects of longshore current variation.

The dispersion mechanism outlined in the present paper, on the other hand, will be

present in all the cases considered both in the laboratory and the field. Under the time varying field conditions the vertical structure of the current profiles may vary substantially with time. The dispersion effect may do the same but remains in effect. All indications suggest that the dispersion will contribute significantly to the horizontal distributions of the current patterns also under field conditions.

One of the consequences is that even in the simple case of the steady uniform longshore current on a straight beach, the three dimensional nature of the flow is an important feature, with the cross-shore circulation providing lateral mixing that exceeds that of the turbulence by an order of magnitude also inside the surf zone.

The turbulence still remains an essential part of the flow since it is the primary agent which through vertical mixing is responsible for shaping the vertical velocity profiles, which then determine the strength of the dispersion.

ACKNOWLEDGEMENTS

The authors gratefully acknowledge important references to the literature from K. Nadaoka and N. Kobayashi. A referee gave suggestions that helped in simplifying the presentation. This work is a result of research sponsored by NOAA Office of Sea Grant, Department of Commerce, under Grant No. NA86AA-D-SG040 (Project No. R/OE-6). The U.S. Government is authorized to produce and distribute reprints for government purposes notwithstanding any copyright notation that may appear herein.

REFERENCES

Battjes, J. A., 1975. Modelling of turbulence in the surf-zone. *Proceedings of a Symposium on Modelling Techniques*, ASCE, San Francisco, pp. 1050–61.

Bowen, A. J., 1969. The generation of longshore currents on a plane beach. *Journal of Marine Research*, 27, pp. 206–215.

Bowen, A. J. and R. A. Holman, 1989. Shear instabilities in the mean longshore current. 1: Theory. *Journal of Geophysical Research*, 94: 18,023–030.

Bowen, A. J. and D. L. Inman, 1974. Nearshore mixing due to waves and wave induced currents. *Rapp. P.-v. Reun. Cons. Int.*, 167, pp. 6–12.

Dodd, N. and E. B. Thornton, 1990. Growth and energetics of shear waves in the nearshore. *Journal of Geophysical Research*, 95, 16,075–083.

Elder, J.A., 1959. The dispersion of marked fluid in turbulent shear flow. *Journal of Fluid Mechanics*, 5, pp. 544–560.

Fischer, H. B., 1978. On the tensor form of the bulk dispersion coefficient in a bounded skewed shear flow. *Journal of Geophysical Research*, 83, pp. 2373–2375.

Harris, T. F. W., J. M. Jordan, W. R. McMurray, C. J. Verwey and F. P. Anderson, 1963. Mixing in the surf zone. *International Journal of Air and Water Pollution*, 7, pp. 649–667.

Inman, D. L., R. J. Tait and C. E. Nordstrom, 1971. Mixing in the surf zone. *Journal of Geophysical Research*, 76, pp. 3493–3514.

Jonsson, I. G. and N. A. Carlsen, 1976. Experimental and theoretical investigations in an oscillatory turbulent boundary layer. *J. Hydro. Research*, 14, 1, 45–60.

Longuet-Higgins, M. S., 1970. Longshore currents generated by obliquely incident sea waves. Parts 1 and 2. *Journal of Geophysical Research*, 75, pp. 6778–6789 and pp. 6790–6801.

Longuet-Higgins, M. S. and R. W. Stewart, 1960. Changes in the form of short gravity waves on long waves and tidal currents. *Journal of Fluid Mechanics*, 13, pp. 481–504.

Longuet-Higgins, M. S. and R. W. Stewart, 1964, Radiation stress in water waves, a physical discussion with application. *Deep Sea Research*, 11, pp. 529–563.

Nadaoka, K., and T. Kondoh, 1982, Laboratory measurements of velocity field structure in the surf zone by LDV. *Coastal Engineering in Japan*, 25, pp. 125–145.

Okayasu, A., 1989, Characteristics of turbulence structure and undertow in the surf zone. Ph.D. Diss., Univ. of Tokyo.

Oltman-Shay, J., P. A. Howd and W. A. Berkemeier, 1989. Shear instabilities of the mean longshore current 2: Field observations. *Journal of Geophysical Research*, 94, pp. 18,031–042.

Putrevu, U. and I. A. Svendsen, 1992. Shear instability of longshore currents: A numerical study. *Journal of Geophysical Research*, 97, pp. 7283–7303.

Svendsen, I. A., 1984. Mass flux and undertow in a surf-zone. *Coastal Engineering*, 8, pp. 347–365.

Svendsen, I. A. 1987. Analysis of surf zone turbulence. *Journal of Geophysical Research*, 92, pp. 5115–24.

Svendsen, I.A. and J. B. Hansen, 1988, Cross shore currents in surf zone modelling. *Coast. Eng.*, 12, 1, 43–62.

Svendsen, I. A. and R. S. Lorenz, 1989. Velocities in combined undertow and longshore currents. *Coastal Engineering*, 13, pp. 55–79.

Svendsen, I. A. and U. Putrevu, 1993. Surf-zone wave parameters from experimental data. *Coastal Engineering.* In press.

Svendsen, I. A., H. A. Schaffer and J. B. Hansen, 1987. The interaction between the undertow and boundary layer flow on a beach. *Journal of Geophysical Research*, 92, pp. 11,845–856.

Taylor, G. I., 1954. The dispersion of matter in a turbulent flow through a pipe. *Proceedings of the Royal Society of London.* Series A, 219, pp. 446–468.

Thornton, E. B., 1970. Variation of longshore current across the surf zone. *Proceedings of the 12th Coastal Engineering Conference*, pp. 291–308.

Thornton, E. B. and R. T. Guza, 1986. Surf-zone longshore currents and random waves: Field data and models. *Journal of Physical Oceanography*, 16, pp. 1165–1178.

Visser, P. J., 1984. A mathematical model of uniform longshore currents and comparison with laboratory data. Communications on Hydraulics. *Report 84-2*, Department of Civil Engineering, Delft University of Technology, 151 pp.

List of Figures

Figure 1

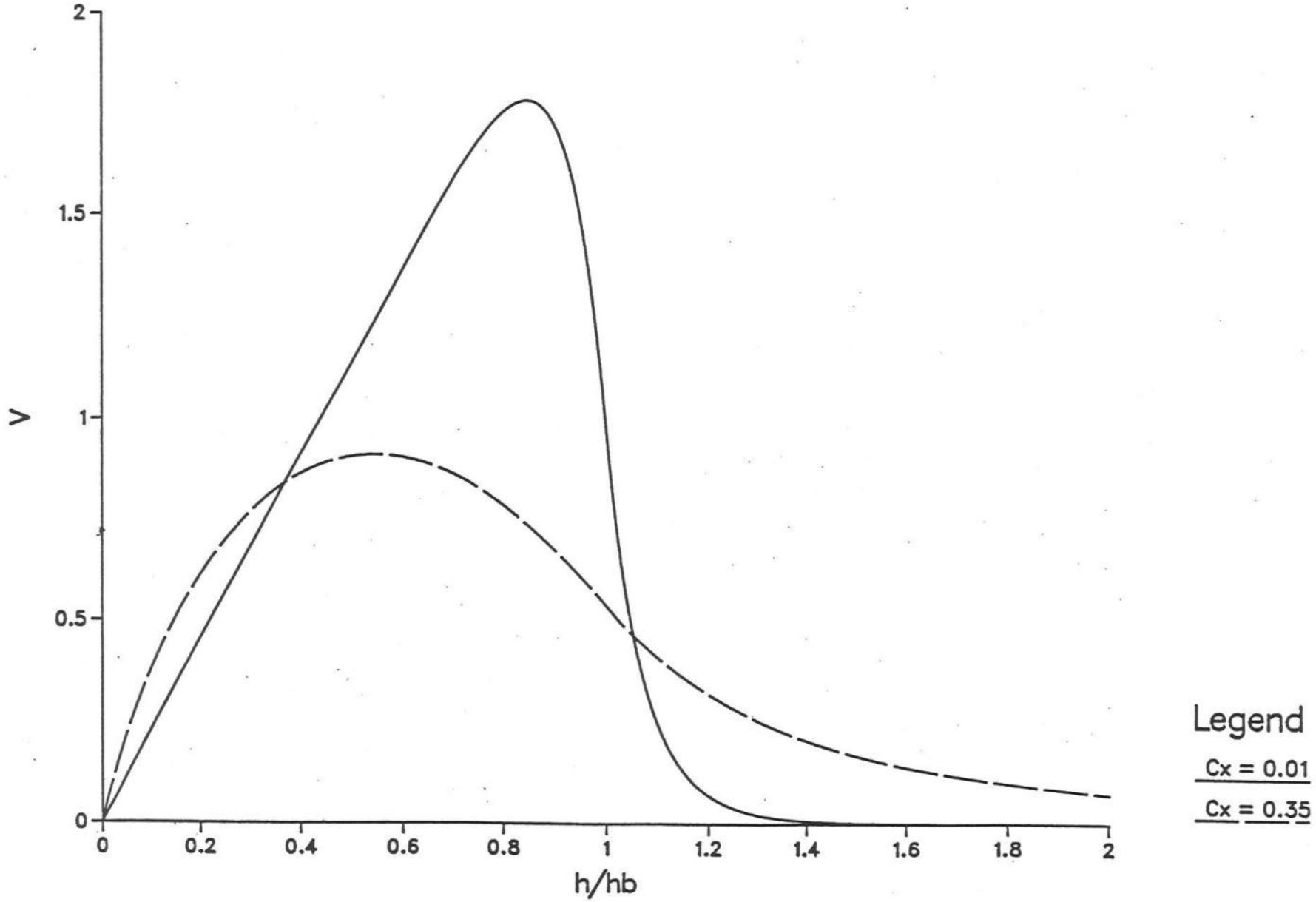

Figure 2

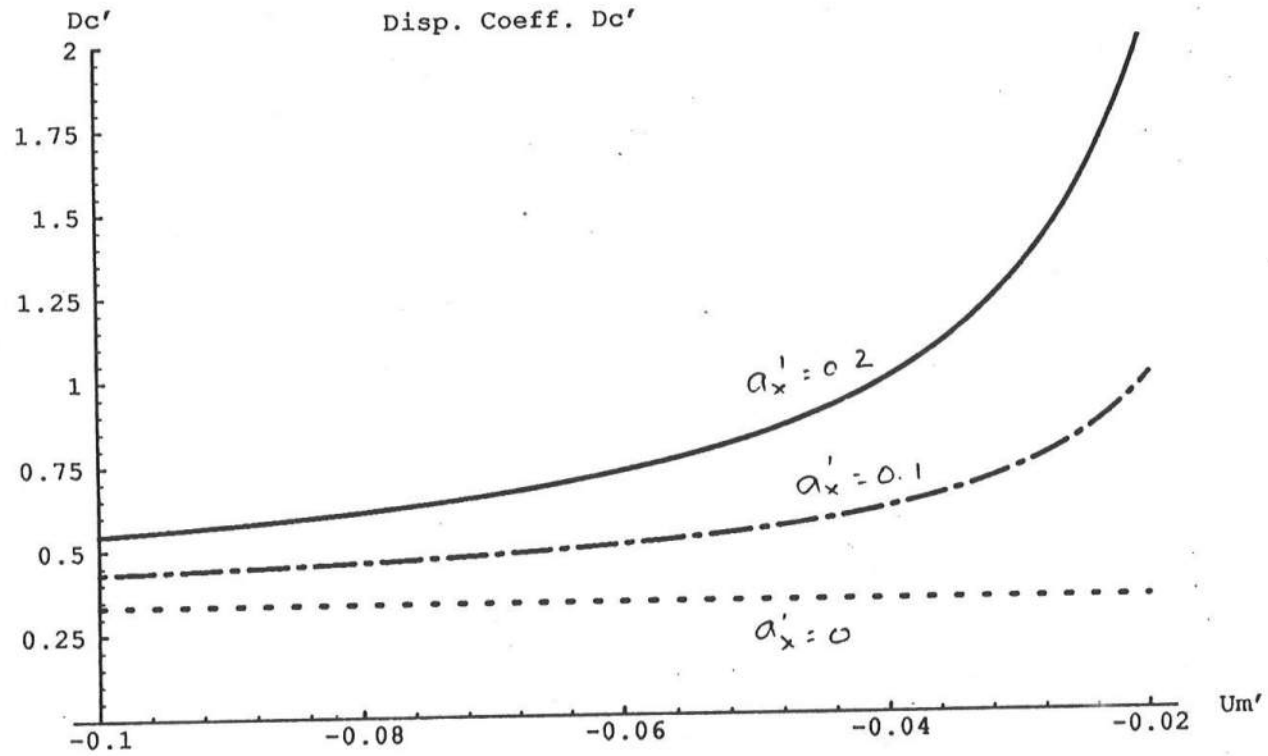
Dc'
Disp. Coeff. Dc'
2
1.75
1.5
1.25
1
0.75
0.5
0.25
$a_x' = 0.2$
$a_x' = 0.1$
$a_x' = 0$
-0.1
-0.08
-0.06
-0.04
-0.02
Um'

Figure 3

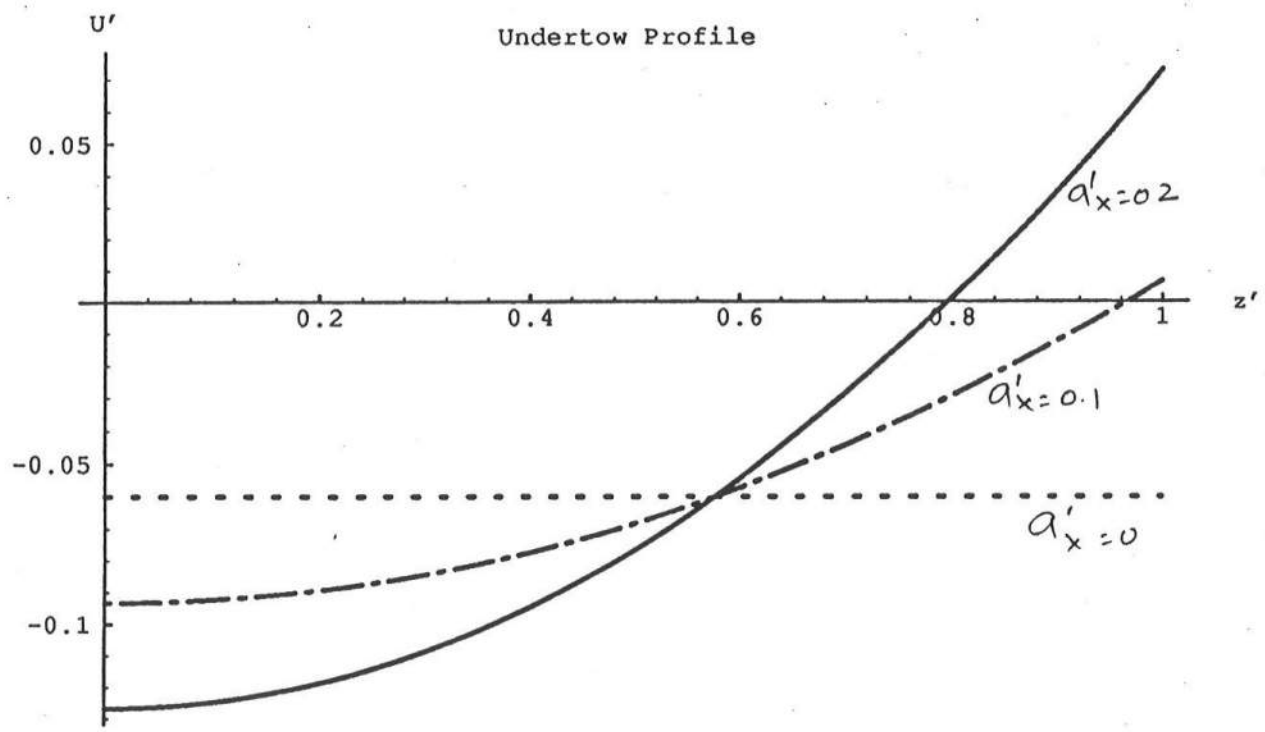

Figure 4

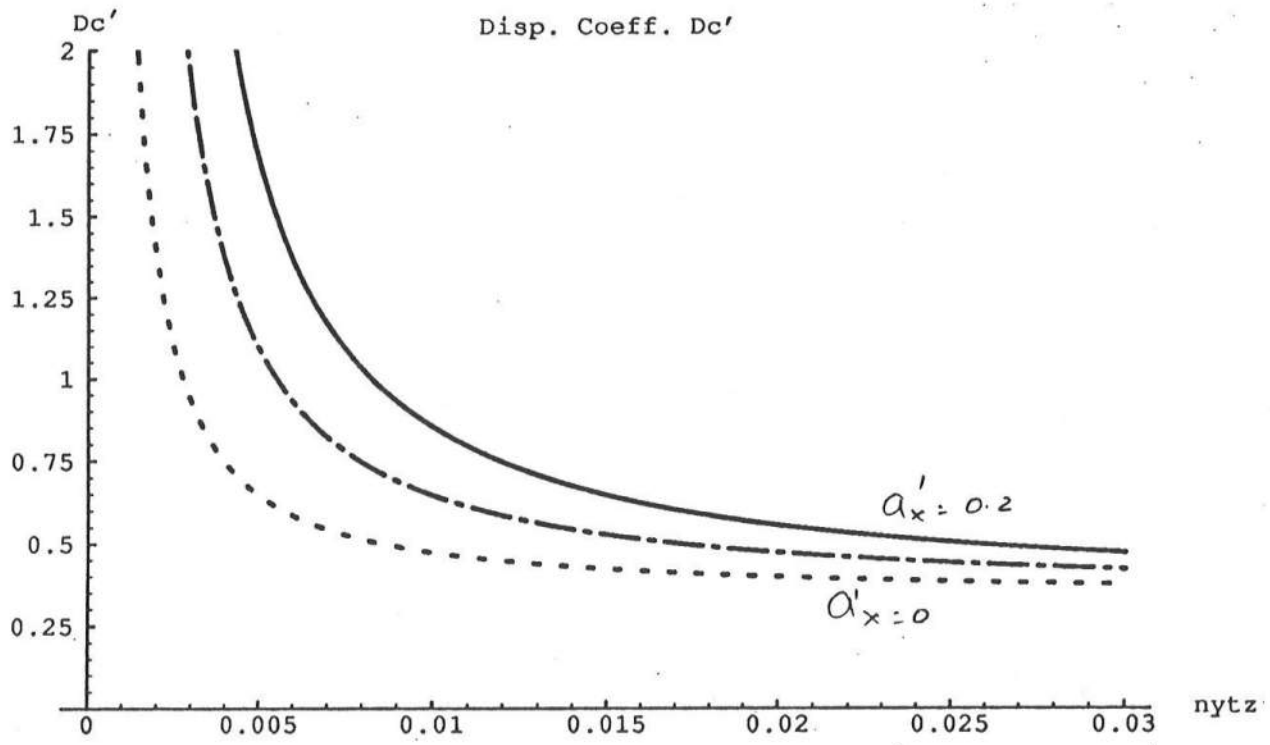
Dc'
Disp. Coeff. Dc'
2
1.75
1.5
1.25
1
0.75
0.5
0.25
0
0.005
0.01
0.015
0.02
0.025
0.03
nytz
$a'_x = 0.2$
$a'_x = 0$

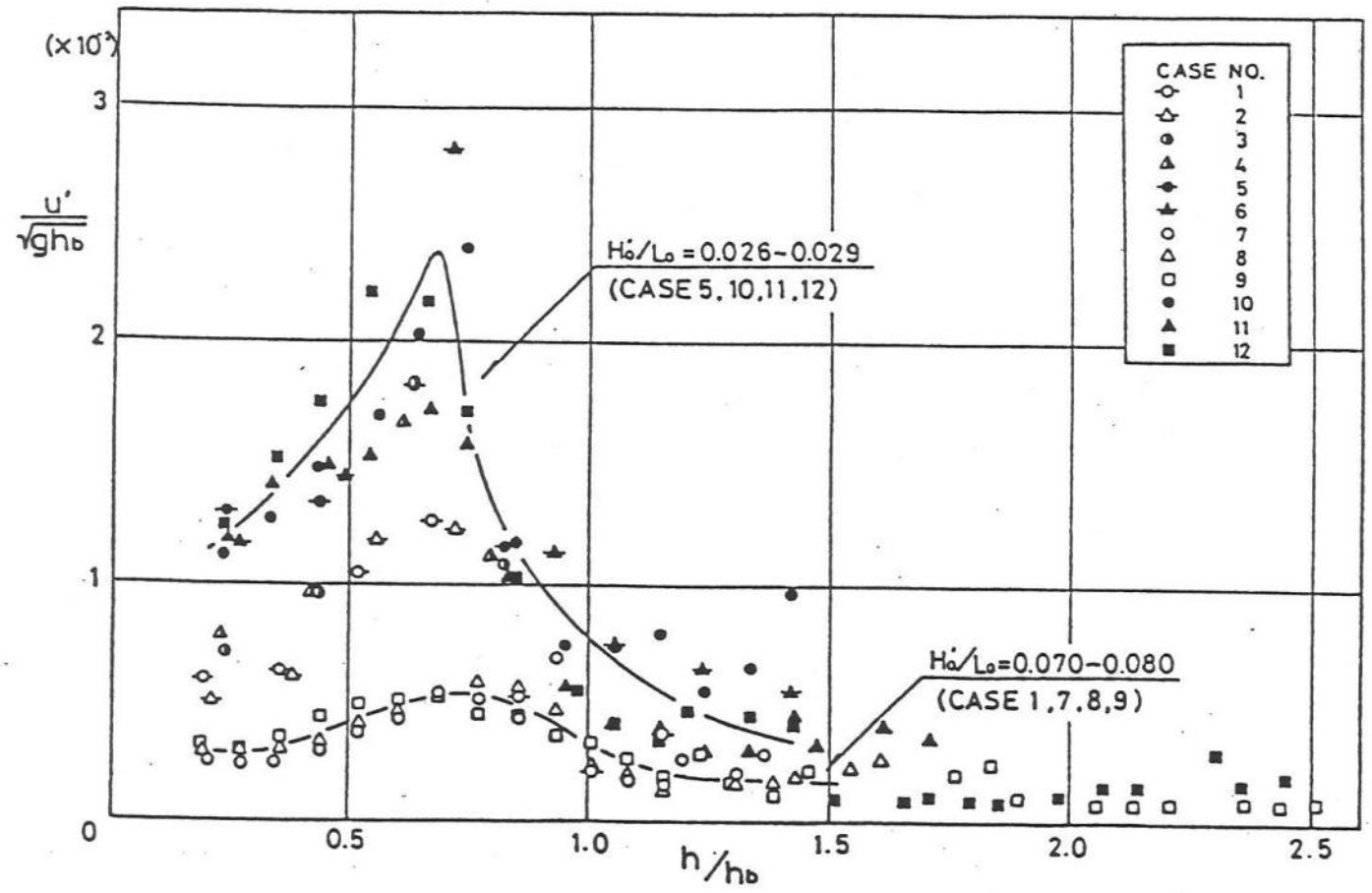
(×10⁻²)
3
2
1
0
u'/√(gh₀)
H₀/L₀ = 0.026~0.029
(CASE 5, 10, 11, 12)
H₀/L₀=0.070~0.080
(CASE 1, 7, 8, 9)
CASE NO.
1
2
3
4
5
6
7
8
9
10
11
12
0.5
1.0
1.5
2.0
2.5
h/h₀

Fig 5

Figure 6

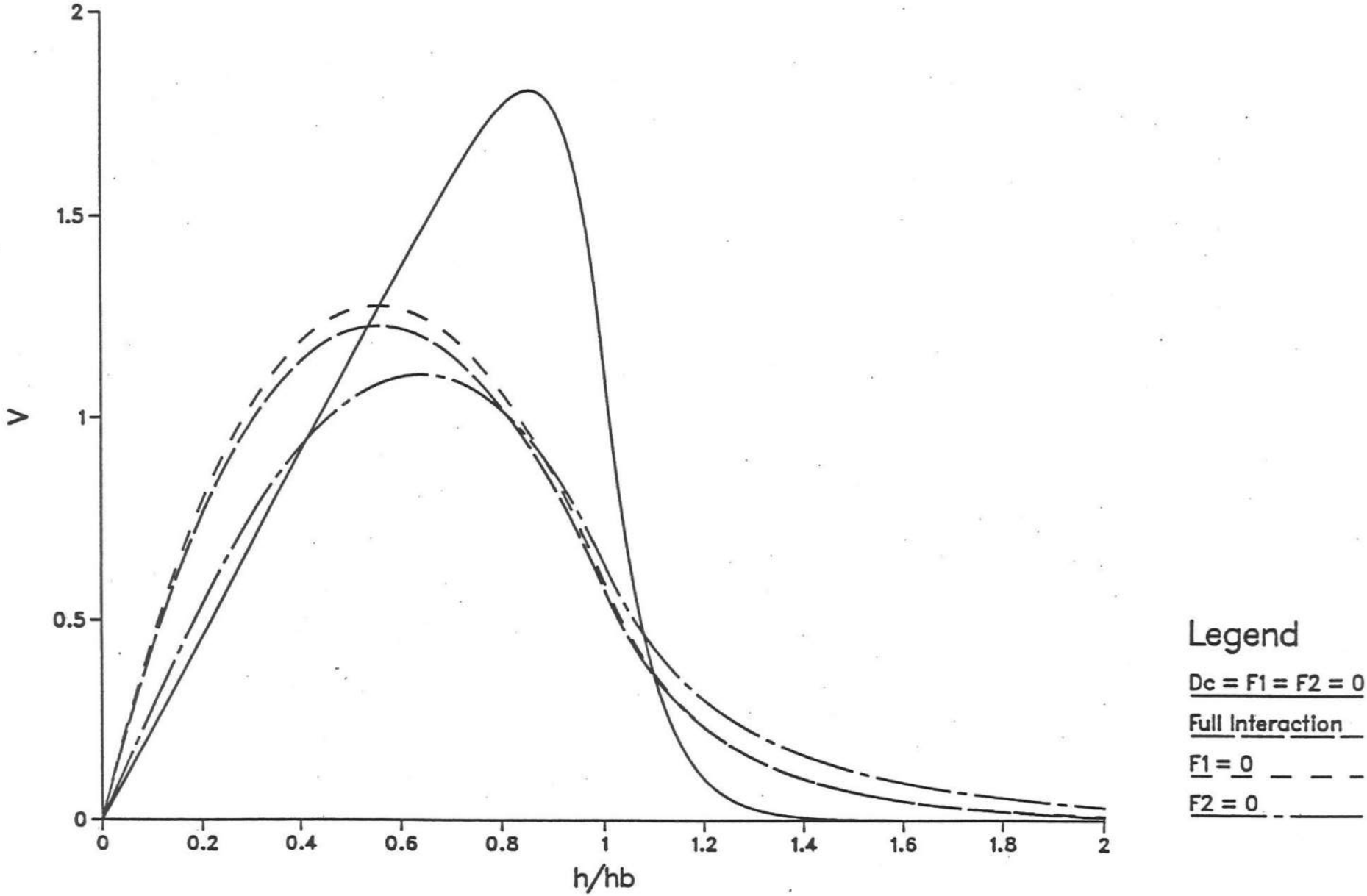
2
1.5
1
0.5
0
V
0
0.2
0.4
0.6
0.8
1
1.2
1.4
1.6
1.8
2
h/hb
Legend
Dc = F1 = F2 = 0
Full Interaction
F1 = 0
F2 = 0

Figure 7

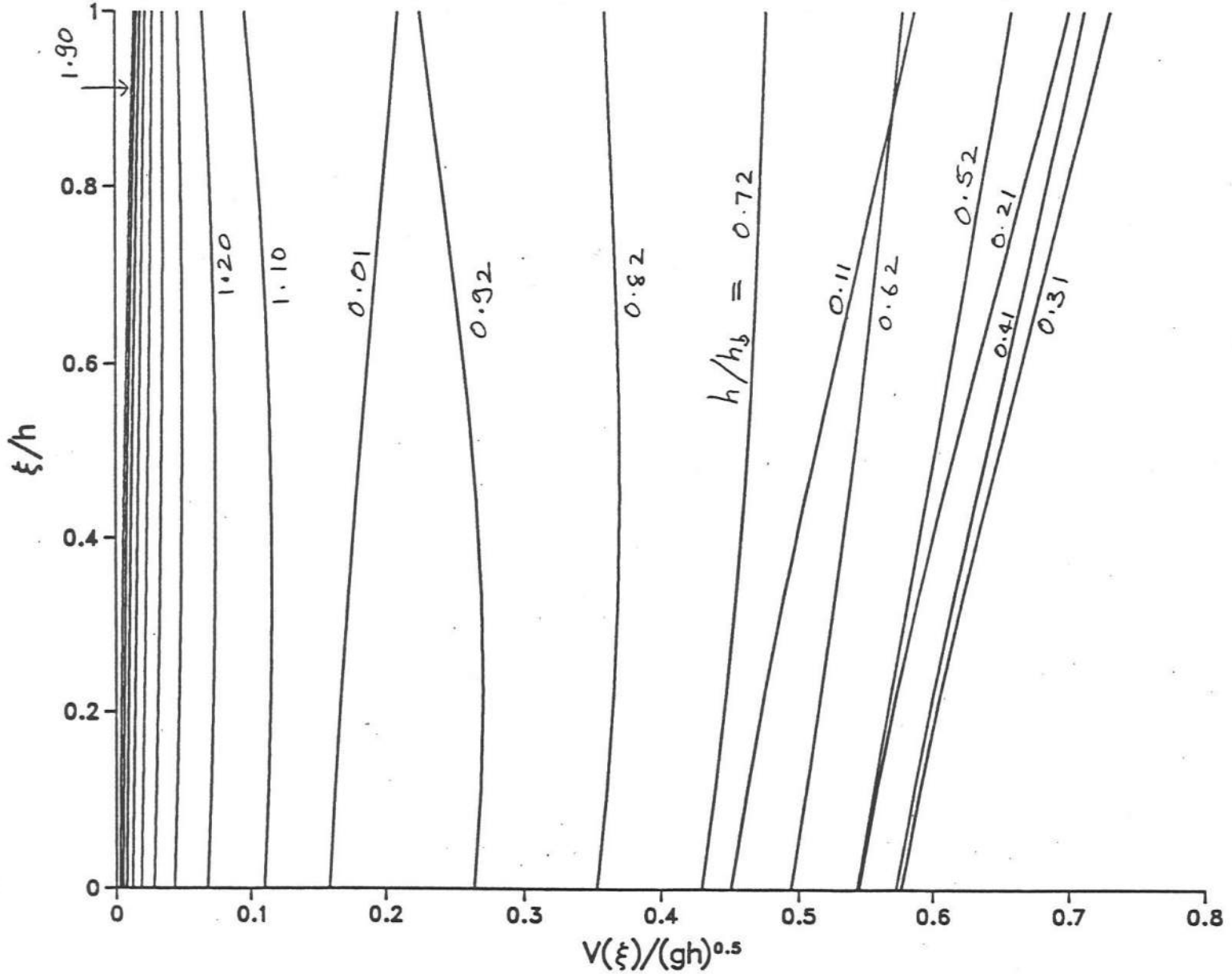

Legend

- h/hb = 0.01
- h/hb = 0.11
- h/hb = 0.21
- h/hb = 0.31
- h/hb = 0.41
- h/hb = 0.52
- h/hb = 0.62
- h/hb = 0.72
- h/hb = 0.82
- h/hb = 0.92
- h/hb = 1.10
- h/hb = 1.20
- h/hb = 1.30
- h/hb = 1.40
- h/hb = 1.51
- h/hb = 1.61
- h/hb = 1.71
- h/hb = 1.81
- h/hb = 1.91

Figure 8

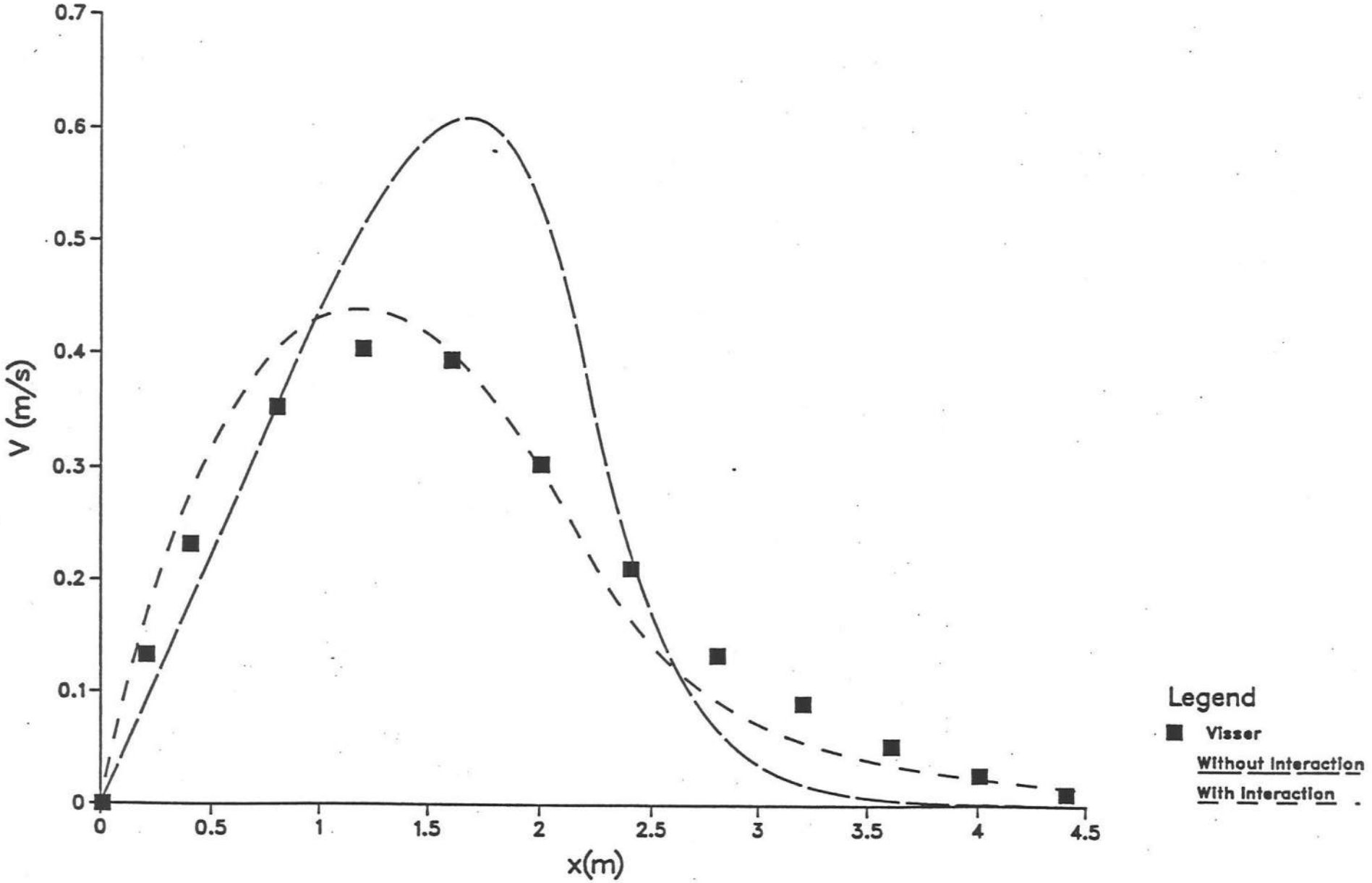
0.7
0.6
0.5
0.4
0.3
0.2
0.1
0
V (m/s)
0
0.5
1
1.5
2
2.5
3
3.5
4
4.5
x(m)
Legend
Visser
Without interaction
With interaction

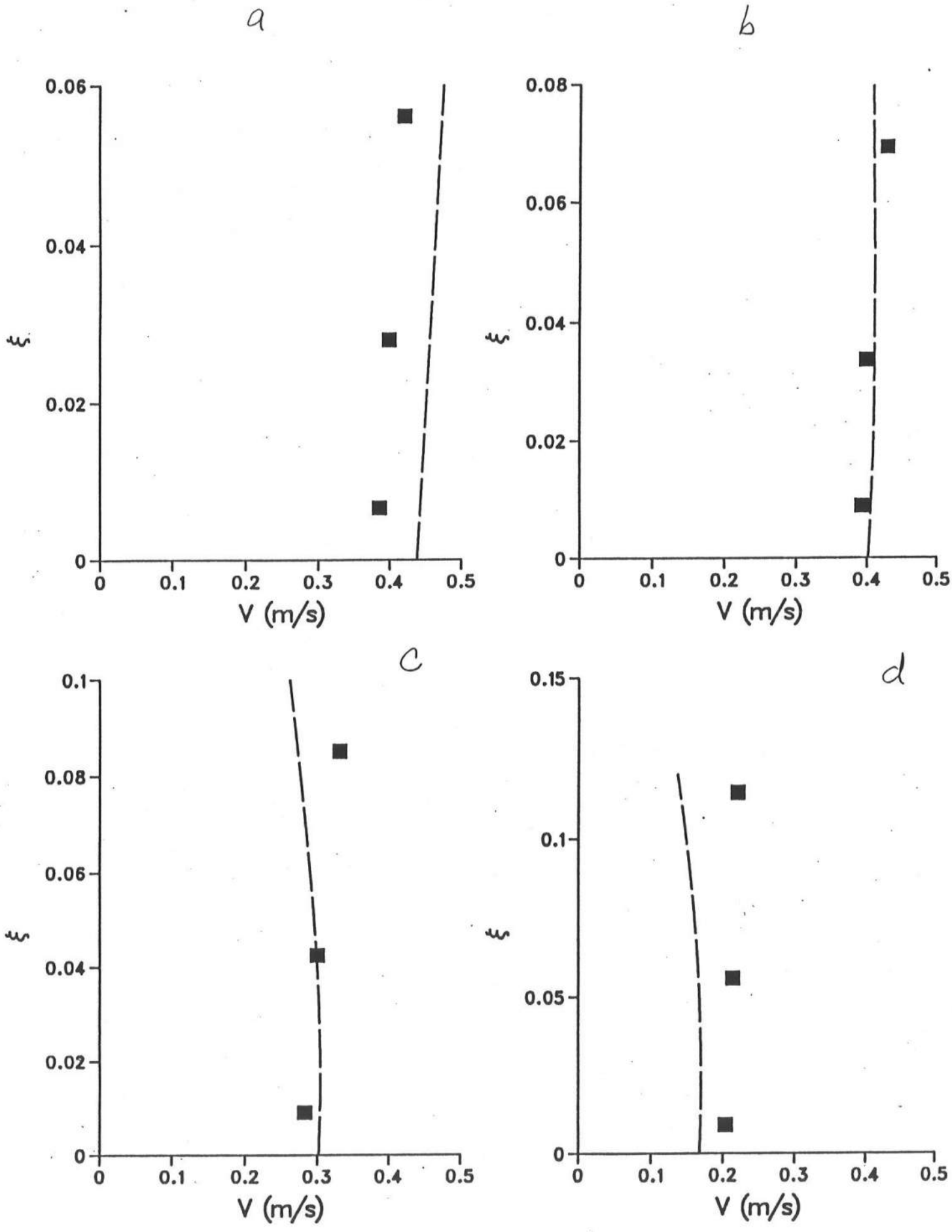

Fig 9 (a - d)

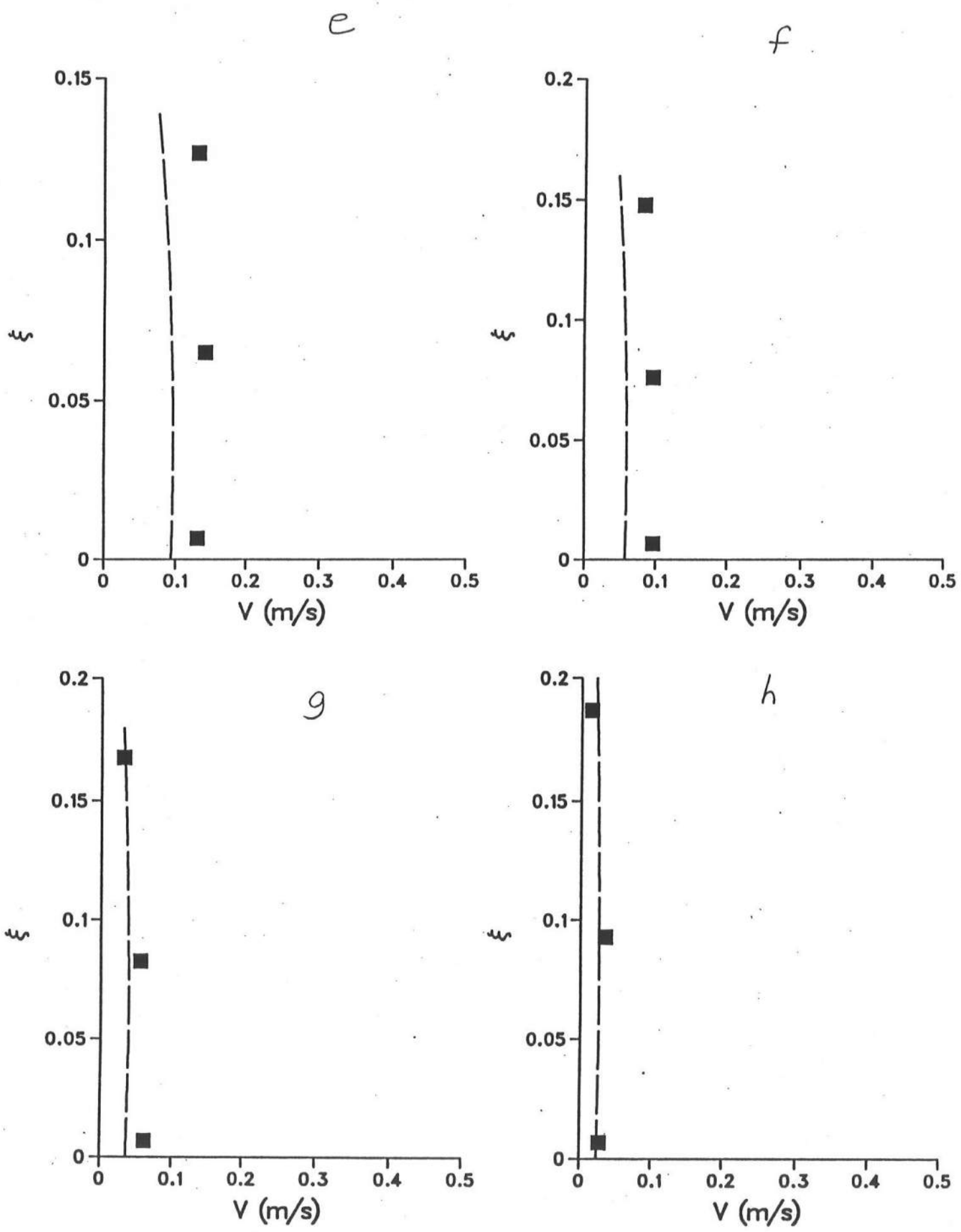

Fig 9 (e-h)